

DOE/NASA/1040-78/1  
NASA TM-78919

# INITIAL TEST RESULTS WITH A SINGLE-CYLINDER RHOMBIC-DRIVE STIRLING ENGINE

(NASA-TM-78919) INITIAL TEST RESULTS WITH A  
SINGLE-CYLINDER RHOMBIC-DRIVE STIRLING  
ENGINE Final Report (NASA) #2 P HC 303/78  
A01 CSCI 10P

N78-31533

Inclas  
63/44 30246

J. E. Cairelli, L. G. Thieme, and R. J. Walter  
National Aeronautics and Space Administration  
Lewis Research Center

July 1978

Prepared for the  
**U.S. DEPARTMENT OF ENERGY**  
Office of Conservation and Solar Applications  
Division of Transportation Energy Conservation

NOTICE

This report was prepared to document work sponsored by the United States Government. Neither the United States nor its agent, the United States Department of Energy, nor any Federal employees, nor any of their contractors, subcontractors or their employees, makes any warranty, express or implied, or assumes any legal liability or responsibility for the accuracy, completeness, or usefulness of any information, apparatus, product or process disclosed, or represents that its use would not infringe privately owned rights.

DOE/NASA/1040-78/1  
NASA TM-78919

**INITIAL TEST RESULTS  
WITH A SINGLE-CYLINDER  
RHOMBIC-DRIVE STIRLING ENGINE**

**J. E. Cairelli, L. G. Thieme, and R. J. Walter  
National Aeronautics and Space Administration  
Lewis Research Center  
Cleveland, Ohio 44135**

**July 1978**

**Prepared for  
U. S. Department of Energy  
Office of Conservation and Solar Applications  
Division of Transportation Energy Conservation  
Washington, D. C. 20545  
Under Interagency Agreement EC-77-A-31-1040**

## SUMMARY

As part of a Stirling-engine technology study for the U.S. Department of Energy, a 6-kW (8-hp), single-cylinder, rhombic-drive Stirling engine has been restored to operating condition, and preliminary characterization tests run with hydrogen and helium as the working gases. The Stirling engine, part of an engine-generator set designated as GPU 3 (ground power unit), was built by General Motors Research Laboratories (GRML) in 1955 for the U.S. Army.

Initial tests at the Lewis Research Center show the engine brake specific fuel consumption (BSFC) with hydrogen working gas to be within the range of BSFC observed by the Army at Fort Belvoir, Virginia, in 1966. The minimum system specific fuel consumption (SFC) observed during the Lewis tests with hydrogen was 669 g/kW·hr (1.1 lb/hp·hr), compared with 620 g/kW·hr (1.02 lb/hp·hr) for the Army tests. However, the engine output power for a given mean compression-space pressure was lower than for the Army tests. The observed output power at a working-space pressure of 5 MPa (725 psig) was 3.27 kW (4.39 hp) for the Lewis tests and 3.80 kW (5.09 hp) for the Army tests. As expected, the engine power with helium was substantially lower than with hydrogen.

## INTRODUCTION

A Stirling-engine-driven ground-power unit (GPU) was obtained from the U.S. Army Mobility Equipment Research and Development Center and restored to operating condition. The entire GPU was tested to obtain Stirling engine performance and operational information. In addition, the Stirling engine dimensions and physical characteristics were measured and defined.

This work was done in support of the U.S. Department of Energy's Stirling Engine Highway Vehicle Systems Program. The Lewis Research Center, through an interagency agreement with DOE's Office of Conservation is responsible for project management of this effort. The intent of the program is to develop the technology needed to pro-

vide the U.S. automobile industry with the option of moving into production engineering for automotive Stirling engines in the mid-1980's.

The Stirling engine driven GPU used in this work was designed and built by General Motors Research Laboratory (GMRL) in 1965 for the U.S. Army. The GPU was tested by the Army in 1966 and then retired. It was obtained by Lewis, restored to operating condition, and installed in a test facility. The tests reported herein were made with helium and with hydrogen as working fluids.

Fuel flow, alternator power output, mean compression-space pressure, heater-tube gas temperature, mean compression-space gas temperature, cooling-water inlet temperature, and several other pressures and temperatures were measured. Engine output power and specific fuel consumption were calculated and compared with the unpublished Army data. The engine's physical characteristics and dimensions, including internal volumes, were determined for use in computer simulation of the engine.

## APPARATUS AND PROCEDURE

### GPU 3 Stirling Ground Power Unit

The GPU 3 electrical power generating unit (fig. 1) was obtained from the Army. A second, identical unit was borrowed from the Smithsonian Institution; it has been used largely as a source of spare parts for the first unit. Both GPU 3 units are self-contained, 3-kW, engine-generator sets built by General Motors Research Laboratories for the Army. The GPU development program is discussed in reference 1, which also includes system performance specifications and some test results. The GPU component development and test results are presented in reference 2.

The GPU 3 units are capable of operating on a variety of fuels and over a broad range of ambient conditions encompassed by the following limits:

Minimum temperature from sea level to 2430 m (8000 ft), °C (°F) . . . . .	4 (40)
Maximum temperature, °C (°F), at -	
Sea level . . . . .	46 (115)
2438 m (8000 ft) . . . . .	32 (90)

Automatic controls, which were an integral part of the engine system, regulated fuel flow to maintain a 677° C (1250° F) hydrogen gas temperature within the heater tubes, and maintained a 3000-rpm engine speed.

### GPU 3 Engine

The heart of the GPU 3 is the Stirling engine, which is capable of producing about 6 kW (8 hp) at a mean compression-space pressure of 6.9 MPa (1000 psig) with hydrogen as the working gas. Figure 2 is a cross section of the GPU 3 engine showing the major internal components. The displacer, rhombic-drive engine was designed to operate with hydrogen as the working gas. The working gas occupies two spaces inside the engine: (1) the working space above the power piston where the thermodynamic cycle occurs and (2) the buffer space below the power piston, which is used to reduce the pressure forces on the mechanical linkages and to minimize piston ring sealing requirements.

The gas in the working space is distributed in three smaller, connected volumes: (1) A compression space at the cold end of the engine bounded by the cylinder wall, the top of the power piston, and the bottom of the displacer piston; (2) an expansion space at the hot end of the engine bounded by the top of the displacer and the end of the cylinder; and (3) a dead space, which includes mainly the internal volume of the heater tubes, the regenerators, and coolers with the connecting passages that tie the compression space to the expansion space.

Strictly speaking, the clearance volumes within the compression and expansion spaces are also considered dead space. Both the com-

pression and expansion volumes are continually varying as functions of the engine crank rotation: As the crank rotates, the variation in these volumes causes the hydrogen working gas to be alternately heated and cooled by the engine's heat exchangers while passing back and forth from the expansion space and the compression space. The total volume occupied by the working gas is also varying as a function of crank rotation. The net work realized for one cycle is the difference between the work produced by expanding hot gas and the work required to compress cold gas.

The effect of dead volume is to diminish the pressure variations during the cycle. Although dead volume is necessary to meet the cycle heat-transfer requirements, it tends to reduce the work produced during one cycle.

Each piston is connected to a shaft, which in turn is connected to two rods, with each rod attached to one of the engine's two crank shafts. The displacer shaft passes through the center of the power piston and piston shaft and attaches to the bottom pair of connecting rods. The power piston shaft attaches to the upper connecting rods. Detailed description and analysis of the rhombic drive can be found in Meijer's thesis (ref. 3).

The following is a brief description of the major engine components and systems. Table I contains details of the engine's internal dimensions.

Cylinder assembly. - The cylinder assembly (fig. 3) contains the cylinder in which both pistons ride, heater tubes, housings for eight cooler-regenerator cartridges, and water-cooling passages that supply water to the coolers and cool the lower cylinder wall. The cover shields and insulation have been removed in figure 3(a) to show the cooler-regenerator housing cylinders and the heater tube connections. Figure 3(b) is an inverted view of the partially assembled cylinder with some of the cooler-regenerator cartridges. The fuel flow control and governor-actuated hydrogen-control valves are also shown. Thermocouples to measure the gas temperature inside the heater tubes and in the passage between the coolers and the compression space are also visible on the left side of the assembly.

Heater tubes. - The eighty Multimet N-155 tubes used are joined at the top of the cylinder assembly to a common header ring; at their lower ends they are alternately connected to either the hot end of the piston cylinder or to the hot end of regenerator-cooler cylinders. The piston cylinder and regenerator-cooler cylinders are made of AISI 310 stainless steel.

Seventy-six of the heater tubes are of the same diameter. The remaining four, located at  $90^{\circ}$  intervals around the cylinder assembly, are of slightly larger diameter and are offset toward the center of the assembly. Each of these larger tubes contains a temperature sensor installed from the bottom of the cylinder assembly. The sensors are used to measure the working-gas temperature inside the heater tubes and to provide a mechanical signal for the temperature controls. Two types of sensors are installed: Thermocouples are used in two of the larger tubes and special bimetallic sensors in the other two.

Figure 4 is a cross section of the bimetallic temperature sensor and fuel-control valve installation. The temperature sensor consists of a stainless-steel tube with a closed end and an inner tungsten rod. Variations in the heater-tube gas temperature causes a change in the length of the outer tube. The length of the inner rod is relatively insensitive to temperature. The relative motion that results between the bottom end of the tube and the bottom end of the rod actuates the fuel control valve.

Cooler-regenerator. - The cooler and regenerator (fig. 5) are fabricated and joined to form a single cartridge. The coolers are miniature shell and tube heat exchangers. Each cooler contains 39, 1.52-mm (0.060-in.) o.d. by 1.02-mm (0.040-in.) i.d. tubes through which the working gas flows. The cooling water makes a single cross-flow pass over the tubes. The cylinder assembly water passages are arranged to form two parallel circuits with four coolers in series.

The regenerators consist of 308 layers of square-weave, 200-mesh,  $40.6\text{-}\mu\text{m}$  (0.0016-in.) wire diameter, stainless-steel screens. The layers of screen are carefully aligned with alternate layers rotated about  $4^{\circ}$  to provide the maximum heat transfer and minimum flow loss. The screens are retained in a thin-walled, electro-deposited, nickel canister,



which is fastened to the cooler by roll forming the edge of the canister into a groove in the cooler. A split ring is placed in the groove to prevent the edge from unrolling when the cartridge is removed from the cylinder assembly. The split ring is not shown in this picture.

The cooler-regenerator cartridges are installed through eight openings around the bottom of the cylinder assembly. Each cartridge is backed by a retainer assembly consisting of (1) a spacer, which provides a connecting passage from the cooler to the compression space, (2) a snap ring to hold the spacer in the cylinder, and (3) a cover plate, which keeps the snap ring in proper position and prevents it from deforming when the engine is pressurized.

O-rings are used to seal the working gas from the cooling water passages. The cross section of the installation is shown in figure 2, and the arrangement of the components in the cylinder assembly are shown in figure 3(b).

Air preheater and combustor assembly. - The air preheater and combustion chamber (fig. 6(a)) are combined in one assembly which mounts on top of the cylinder assembly.

The counterflow preheater is made of vertical rows of horizontal tubes separated by vertical baffles. The tubes and baffles are arranged in spiral fashion radiating from the inside diameter of the preheater to its outside diameter. The entire assembly is made of stainless steel.

Figure 6(b), a cross section through the preheater-combustor assembly, indicates the airflow path through the preheater and combustor. Air enters the bottom of the preheater on the outside diameter. A plenum chamber distributes the air around the base of the preheater. The air is then distributed vertically through 16 passages which serve as headers. Then it flows between the baffles picking up heat from the tubes as it flows inward along a spiral path. Another set of 16 passages at the inside diameter collect the heated air and channel it to a plenum at the top of the preheater. This plenum feeds the heated air into the combustion chamber. The hot exhaust enters the tubes at the inner diameter of the preheater and flows outward on a spiral path to an annular space at the outer diameter of the preheater and then upward through the end of the

annulus to the atmosphere. This preheater configuration is one of several investigated by GMRL. These are discussed in some detail by Percival (ref. 2).

The combustion chamber is mounted inside the preheater. Fuel is atomized by the fuel nozzle through use of a separate atomizing air circuit fed by two small, vane type air pumps. The atomized fuel is mixed with the preheated combustion air and is burned in the combustion chamber. A special spark plug is provided to initiate combustion. Once combustion is started, the spark plug is deenergized. Burner design and development are discussed in reference 2. GPU 3 exhaust emissions with and without exhaust-gas recirculation were reported by researchers at Wayne State University (refs. 4 and 5).

Pistons, shafts, and seals. - Figure 7 shows the displacer and power pistons assembled with their respective shafts, which are connected to the rhombic-drive mechanism through the power-piston and displacer-piston yokes. Both shaft seal assemblies are also shown. The displacer shaft passes through the hollow power-piston shaft. The displacer shaft is tinplated at its lower end and is connected to its yoke with an interference fit to insure that the shaft is perpendicular to the centerline of the displacer yoke pins. This is necessary to insure shaft seal alignment. The power piston is attached to its yoke with a hollow pin. This allows the driving force to be divided equally between the two crank shafts, while allowing the shaft to be guided by a bushing just below the power-piston seal.

Shaft seals. - The GPU 3 engine uses sliding seals on both the displacer and power-piston shafts. Figure 7 shows the cross section through the seals, and figure 8 is a photograph of the displacer shaft and its seal parts.

The shaft seals for the GPU 3 were made by GMRL using their own Buna-N (nitride) formulation. The seal has a T-shaped cross section and uses phenolic antirolling shields (backup rings) on either side. The design of the seal is very similar to the Palmetto GT seal manufactured by Greene Tweed & Company.

A Disogrin rod wiper is installed below each seal to help prevent crankcase oil from passing through the rod seals. To insure rod

alignment with each seal, a Glacier "DU" guide bushing is located between the seal and the wiper. In the lower seal assembly, a spring loaded Teflon cap seal is mounted above the T-seal to reduce the pressure differential across the power-piston seal. The cap seal is mounted so that it acts as a check valve, allowing flow out of the space between seals thereby exposing the T-seal to a relatively constant pressure approximately equal to the minimum buffer-space pressure.

Later versions of the GPU 3 engine made use of rollsock seals similar to those used by N. V. Philips. The seal work done at GMRL is described in reference 2.

Piston seal rings. - The piston seal rings are shown in cross section in figure 7. Figure 9 is a photograph of the GPU 3 pistons and a set of piston rings. The seals for the displacer piston and power piston to the cylinder is accomplished using square-cut, Rulon LD piston rings. The rings are made up of an inner and an outer ring. The inner ring, which has square ends having a metal-coil-compression spring set into the end gap, expands to force the outer ring against the cylinder wall. The outer ring has a stepped end gap. The two rings are kept in alignment by a small metal pin so that the end gaps are  $180^{\circ}$  apart. Two sets of piston rings are used on each piston. The rings are radially grooved on one face. Each set of rings is installed with the grooves facing the other set. The grooves cause the rings to act as check valves thereby tending to build up pressure in the space between the rings. This pressure exerts a radial force on the rings and improves their sealing capacity. On the displacer piston the upper rings are smooth (not grooved) to prevent hot gas flow past them.

Engine oil system. - The engine oil system supplies oil for lubrication as well as the energy for operation of the engine controls. A positive displacement pump geared directly to one of the output shafts supplies oil at about 0.4 MPa (60 psig). A straight SAE 10W oil, without additives, is used to minimize deterioration of the elastomeric seals. This system is somewhat complex and since it is not pertinent to our discussion of the basic Stirling engine, it will not be given any further discussion.

Engine controls. - Control of the GPU 3 is accomplished through unique hydromechanical devices. Two independent control systems are used: one to maintain nominal heater temperature at  $950^{\circ}\text{C}$  ( $1250^{\circ}\text{F}$ ) and one to maintain engine speed at 3000 rpm. Both controls have manual adjustments to change the set point within a narrow range. Safety devices are also provided to override the normal controls in the event of heater overtemperature or engine overspeed.

Heater-tube temperature control. - Figure 10 is a greatly simplified schematic diagram of the heater-tube temperature control. Bimetallic temperature sensors are mounted within two of the special, larger-diameter heater tubes. (See section Heater tubes.) The position of the rod protruding from the bottom of each sensor is proportional to the heater-tube gas temperature. One of the bimetallic sensors mechanically positions the gas temperature-controlled fuel valve, thereby controlling the fuel flow. As the temperature rises toward the desired heater-tube gas temperature ( $950^{\circ}\text{C}$ ,  $1250^{\circ}\text{F}$ ), the fuel flow rate drops; as the temperature drops from the desired temperature, the fuel flow rate rises. The second bimetallic sensor actuates the fuel cutoff valve: If the heater-tube gas temperature exceeds  $990^{\circ}\text{C}$  ( $1320^{\circ}\text{F}$ ) this valve closes the control oil supply line causing the shutoff valve to close and the engine to make a normal stop.

Speed control. - Figure 11 is a simplified diagram of the speed-control system. Hydrogen gas, sufficient to supply the needs of the GPU for extended operation, is stored in a high-pressure tank. The tank is initially charged to about 13.8 MPa (2000 psig). A supply pressure regulator within the hydrogen-control manifold limits maximum hydrogen supply pressure to the engine to 6.9 MPa (1000 psig).

A flyball governor is used to sense engine speed. The governor regulates the control-oil pressure, which actuates the governor-actuated hydrogen valve. If the engine speed is below 3000 rpm, the governor causes the valve to increase the pressure in both the compression and buffer spaces by allowing flow from the high-pressure storage tank to the engine. If the speed is too high, the governor causes the valve to vent both engine spaces to the hydrogen compressor,

which pumps the hydrogen back into the high-pressure storage tank. Since the hydrogen compressor capacity is not adequate to reduce engine power quickly, the governor-actuated hydrogen valve provides a bypass between the working space and buffer space to assist governing during sudden load decreases.

An overspeed device is built into the speed governor. It prevents operation at speeds above 3450 rpm. If this speed is exceeded, the control-oil pressure to the hydrogen overspeed bypass valve is cut off. This opens the valve, reducing the engine power, and prevents further increase in speed. In addition, control-oil pressure is dumped, thus causing the fuel flow to be cut off and the engine to come to a normal stop.

Auxiliary systems. - Several auxiliary components are grouped and mounted in one assembly (fig. 12(a)). These include the combustion air blower, two vane type fuel-atomizer air pumps, the magneto, and fuel pump. They share a drive system which is powered by either of two methods: (1) a pulley on the front of the engine through an over-running clutch or (2) the hand starting crank. To insure adequate air-flow, both atomizer pumps are driven during startup. But only one operates when driven by the engine. The cooling-water pump (fig. 12(b)) and radiator fan (fig. 12(a)) are driven directly from a pulley on the front of the engine. These rotate only when the engine output shaft is rotating. A tachometer to read engine rpm and an engine total-runtime meter were also included with the original unit. Figure 12(b) shows the gages and meters installed on the GPU 3 as it was received at Lewis.

Engine startup system. - Although earlier versions of the GPU used an electric starter, the GPU 3 is started by hand. This change was made to reduce its weight. A hand crank located at the alternator end of the unit (fig. 12(a)) is used initially to rotate the engine to place the power piston at top dead center (TDC) thus positioning the engine at the beginning of the expansion stroke. Once the power piston is properly positioned, the crank is used to rotate the combustion air blower, fuel atomizing air pumps, fuel pump, and spark magneto. This provides the means to warm up the heater tubes. Selection of the

function of the hand crank is made by manual engagement of either of two hand clutches (not visible in the figures). The power-piston positioning mechanism disengages automatically when the power piston is at TDC. The gearbox clutch is disengaged automatically when the engine takes up the torque load for the auxiliaries drive.

When the gas temperature in the heater tubes is at the normal operating temperature of 950 K (1250<sup>o</sup> F), the starting pull cable (fig. 12(b)) is pulled. The pull cord, which is attached to a recoil mechanism similar to those used on lawn mowers, rotates the crank shafts and moves the pistons. As the engine speed builds, the combustion system drive is taken over by the engine through the overrunning clutch, the gearbox clutch disengages, and the hand cranking is discontinued.

### Instrumentation

The GPU 3 Ground Power Unit came to Lewis fitted with Bourdon tube pressure gages, electrical meters, and thermocouples. Table II lists the parameters measured, the type of instrument used and the range of reading. The pressures were read on separate gages. The thermocouples were read on two meters, one for heater-tube gas temperature and one for the remaining temperatures. The thermocouple to be read on the second meter was determined by positioning a selector switch.

Figure 13 shows the GPU 3 as it was tested at Lewis. Table III lists the instrumentation added to the GPU 3, its type and range. Several pressure gages were relocated to the gage panel on the operator side of the unit. (All instrumentation used during these tests read in U.S. Customary units.)

### Test Setup

The test setup for the testing of the GPU 3 is shown in figure 14. Although our interests are primarily with the engine, the complete GPU 3 unit, with only minor modification, was tested to minimize the

facility support systems. Some modification was required to circumvent operational problems and facilitate testing. The following changes were made to the GPU 3 for the initial tests.

(1) Two externally mounted fuel tanks with nitrogen pressurization were substituted for the original self-contained tank and fuel pump. These tanks were connected to the engine through a selector valve which allowed use of the smaller tank for startup and between data points, and use of the larger during the gathering of data. This was done to provide a means for determining the fuel consumption. The fuel tank used during the data runs is shown in figure 14 on the lower level of the test stand on the right hand side.

In addition, chronic malfunction of the temperature control made it necessary to install a manually adjusted needle valve in the nozzle fuel line. The overtemperature fuel cutoff system appeared to operate and was left intact. The fuel-control needle valve is shown in figure 13 on the upper gage panel.

(2) The high-pressure-hydrogen tank (see fig. 13) was not used. An external, gas-supply panel was made up to control the supply of either hydrogen or helium directly to the hydrogen-supply regulator on the hydrogen-control manifold. The gas supply panel is shown on the right of the test stand in figure 14. The hydrogen compressor was disconnected, and the hydrogen vent, which would normally be connected to the compressor, was tied directly to an atmospheric vent.

(3) A leak developed in the original oil cooler, which was located inside the cooling-water radiator. To avoid complicated repair, an external oil cooler was installed in front of the water radiator. The connections to the original oil cooler were capped to prevent loss of coolant.

(4) The alternator output power was absorbed by the separate resistance load bank shown at the left of figure 14. Engine load was changed by varying the resistance of the load bank. A voltage regulator mounted on the GPU maintained the voltage at 30 volts. The regulator was not altered for these tests.

ORIGINAL PAGE IS  
OF POOR QUALITY.

(5) A hood was installed over the generating unit to prevent hydrogen accumulation as well as to remove the combustion products from the test area.

Figure 15 is a simplified schematic diagram of the GPU 3 test setup. It shows the major engine components and indicates the instrumentation used during the tests.

### Test Procedure

The GPU 3 was installed in the test stand (fig. 14), and the various systems and instrumentation were connected (fig. 15). The hydrogen or helium supply was set. The engine was then purged of air by alternate pressure-vent cycles of the working and buffer spaces, first with helium and then with hydrogen, if hydrogen was to be the working fluid. The fuel tanks were filled with No. 1 diesel fuel. The run tank was weighed, and then both tanks were pressurized to about 1.86 MPa (27 psig) with nitrogen gas. The startup tank was valved to the engine. The electrical load on the alternator was set at zero.

The engine was then rotated using the hand crank to position the power piston at top dead center. The control-oil pressure accumulator, which is contained in the control oil manifold, was then pumped up using the small hand-actuated pump, also located on the control-oil manifold. The engine was then pressurized with helium or hydrogen gas to about 3.45 MPa (500 psig).

Next, the combustion system was started. The manual clutch in the gearbox was energized, and the hand crank rotated to start the combustion-airflow and spark. Fuel flow was controlled by adjusting the fuel needle valve. When the heater-tube temperature reached approximately 704<sup>o</sup> C (1300<sup>o</sup> F), the pull cable was pulled, and the engine began rotating. Once the engine attained sufficient speed to overtake the overrunning clutch, the cranking was stopped. The engine pressure control was then allowed to operate normally with the speed governor. The engine speed increased to the normal 3000 rpm. Warmup to normal operating temperatures required about 15 minutes. The resistance of



the load bank was then adjusted to load the engine as desired. The speed-governor system automatically adjusted engine pressures to maintain constant 3000 rpm. The heater-tube gas temperature was controlled manually by adjusting the fuel needle valve. When necessary, the speed governor was adjusted to the correct speed. The engine was allowed to stabilize for about 15 minutes. The run fuel tank was then valved to the engine and the time noted. A data reading was taken of alternator voltage and current and of all other instruments after 5 minutes had passed. A second reading was taken after 10 minutes. After 15 minutes the fuel supply was switched back to the startup tank. The fuel tank was then weighed on the balance scale. The amount of fuel used was determined by comparing the initial and final weights of the tank. This procedure was repeated for each data point. A series of load points were run at 3000 rpm with helium as the working fluid and then with hydrogen. The heater-tube temperature was maintained at  $677^{\circ}\text{C}$  ( $1250^{\circ}\text{F}$ ) for all testing.

The indicated heater-tube-gas temperature varied slightly because of the method of control but never was farther than  $\pm 5.6^{\circ}\text{C}$  ( $\pm 10^{\circ}\text{F}$ ) from  $677^{\circ}\text{C}$  ( $1250^{\circ}\text{F}$ ) for all data points.

The cooling-water temperature was not controlled. For the helium tests the cooling-water-inlet temperature ranged from  $27^{\circ}$  to  $43^{\circ}\text{C}$  ( $80^{\circ}$  to  $109^{\circ}\text{F}$ ). The water temperature tended to increase as the alternator load increased. The thermocouple used to monitor the water-inlet temperature failed to operate during the hydrogen testing; therefore, it was not recorded during that portion of testing.

## RESULTS AND DISCUSSION

The results of the initial GPU 3 tests with helium or hydrogen as the working gases are presented in two ways: (1) those related to the overall engine-generator system and (2) those related to just the engine. Our data are compared with heretofore unpublished Army data taken in 1966. Selected data from the Lewis tests are listed in tables IV and V; Army data are given in the appendix (p. 19). Both the Lewis

and the Army data contained in these tables were originally read in U.S. Customary units; they have been converted to the SI System for reporting purposes. All of the Lewis data were obtained with the alternator loading the engine. Since most of the Army testing was done to verify system endurance, only a small portion of their data, representing the extremes in GPU 3 performance, are presented. These data include two sets of data with alternator and one set with the engine loaded with a dynamometer. The maximum power absorbing capability of the alternator is about 3 kW (5 hp). The Army dynamometer test data showed the engine to be capable of producing 5.97 kW (8 hp). The overall GPU 3 system results are presented in figures 16 and 17.

Figure 16 shows the alternator output as a function of mean compression-space pressure. Curves of Lewis data are plotted for both helium and hydrogen. Two sets of Army hydrogen test data are also plotted for comparison. The maximum alternator output of 2.59 kW (3.48 hp) with hydrogen occurred at 5.00 MPa (725 psig). The maximum alternator output with helium at about the same pressure was 1.33 kW (1.79 hp), or about half the hydrogen output. The pressures for the no-load condition (1.76 MPa (255 psig) for hydrogen and 2.69 MPa (390 psig) for helium) indicate that a considerable portion of the power is needed to drive the engine auxiliaries and to overcome windage and friction.

The Army data with hydrogen indicated higher alternator output for a given mean compression-space pressure than the Lewis data. This was the case over the entire operating range. At 4.90 MPa (710 psig) the output during the army tests was about 3 kW (4 hp) or about 0.45 W (0.6 hp) above that measured in the Lewis tests with hydrogen. The lower output power for the same pressure is probably due to excessive leakage past the power piston rings. A new piston had been made after the discovery of a crack in the original piston. Through an oversight, the new piston was made according to the latest revised drawing rather than as originally fabricated. As a result, the ring grooves were made too wide. An attempt to salvage the piston by

repairing the ring grooves resulted in a poor surface finish on the faces on which the ring was to seal. Another factor that may have contributed to the lower power was the deterioration and partial blockage of the regenerators.

Figure 17 shows the overall system SFC with alternator output for hydrogen and helium. The minimum SFC with hydrogen was 669 g/kW·hr (1.1 lb/hp·hr) and occurred at slightly less than 2.4 kW (3.2 hp). The Army tests yielded slightly higher SFC over most of the power range. At about 2.6 kW (3.5 hp) the SFC's for both tests were about 670 g/kW·hr (1.1 lb/hp·hr). Minimum SFC observed by the Army was 623 g/kW·hr (1.02 lb/hp·hr) at 3 kW (4 hp). The Lewis tests were run with heater-tube gas temperature between 671° and 682° C (1240° and 1260° F) and cooling-water temperatures from 27° to 43° C (80° to 110° F). The Army tests of June 1966 were run with the heater-tube gas temperatures between 649° and 666° C (1200° and 1230° F) and with the cooling-water temperatures ranging from 48° to 56° C (118° to 132° F). The July 1966 army tests were conducted with the heater temperature lowered to between 593° and 607° C (1100° and 1125° F) with the cooling-water temperatures ranging from 46° to 60° C (115° to 140° F).

The Carnot efficiencies determined by these temperatures are consistent with the ranking of the system SFC observed in the Lewis and Army tests. However, the relative values of SFC appeared to be more sensitive to the operating temperatures than would be predicted by the relative Carnot efficiencies.

The data required to make a detailed heat balance were not taken; therefore, it is not possible to determine how much of the difference in SFC could be attributed to operating temperature and how much to the difference in parasitic load caused by removal of the fuel pump and hydrogen compressor in the Lewis tests. Although neither of these parasitic loads is a large power consumer, their removal may have produced the same order of magnitude SFC changes as the operating temperatures.

The minimum SFC with helium was 1274 g/kW·hr (2.1 lb/hp·hr) at about 1.3 kW (1.8 hp). It appears that the SFC could be even lower

at a higher alternator output, but the limitation of the operating pressure precluded further testing.

This represents a 39 percent increase in SFC over the SFC for hydrogen at 1.3 kW (1.8 hp). The Lewis computer model (ref. 6), which does not include combustion or mechanical losses, indicates that the SFC with helium should be about 12 percent higher than the SFC with hydrogen.

Recently acquired, previously unpublished GMRL reports indicate that the GPU 3 performance with helium was far below that predicted by their engine analysis program. They found that the piston-ring friction was affected by the working gas. When using the same set of piston rings in the test rig and changing only the gas, the power required to drive the rig with hydrogen and nitrogen was the same, but more power was required to drive the rig with helium.

The engine brake horsepower was calculated from the alternator output by making use of alternator efficiency data also obtained from the Army. Figure 18 shows alternator efficiency at 3000 rpm with the output voltage regulated to 30 volts.

Figure 19 shows the engine brake output power as a function of mean working pressure for both helium and hydrogen. The range of Army data for hydrogen is also plotted for comparison. The upper boundary of the Army data is dynamometer data taken in February 1966; the lower boundary is alternator data obtained in July 1966. The engine power in the Lewis tests fell slightly below the range for the Army tests. The maximum output with helium was 1.68 kW (2.25 hp) and with hydrogen 3.27 kW (4.39 hp). Both maximums were obtained at a mean compression-space pressure of about 5 MPa (725 psig). The difference in brake horsepower between operating with helium and operating with hydrogen was 1.60 kW (2.14 hp). The Lewis computer model predicted a 1.42-kW (1.9-hp) decrease in power when operating with helium. The maximum power from the Army test data, using a dynamometer load, was 6 kW (8.04 hp) at a mean compression-space pressure of 6.9 MPa (1000 psig) and heater-tube gas temperatures from 680° to 706° C (1256° to 1302° F).

The engine BSFC's with hydrogen and with helium are shown in figure 20 as a function of engine brake output. Comparison is made with the range of BSFC observed during the Army tests. The BSFC observed during the Lewis tests with hydrogen tended to fall within the range of the Army data, as would be expected from the operating temperatures. The Lewis helium data tended toward the upper limits of the range of Army data. The higher fuel consumption with helium gives some indication of the increase in internal windage losses.

### CONCLUDING REMARKS

This limited investigation provides some of the dimensional and experimental information needed to evaluate a computer model of a Stirling engine. This work is expected to continue so as to provide a body of Stirling-engine test data for validation of computer models, such models to provide the basis for formulation of specific design criteria for advanced Stirling engines.

As presently planned, the GPU engine will be reworked into a research engine configuration. Auxiliary components such as the combustion air blower, fuel pump, and so forth will be removed and replaced with facility items. Engine components, such as the cooler-regenerators, that are worn will be replaced. The engine will be extensively instrumented.

Future work may also include testing of advanced component concepts. The GPU engine testing will continue until a more suitable research tool is available. Such a tool, the Stirling general purpose test engine, is now being designed.

## APPENDIX - ARMY TEST DATA

TABLE A-I. - DYNAMOMETER TESTS OF FEBRUARY 1966

[Working fluid, hydrogen; operating speed, 3000 rpm; fuel, JP4; fuel lower heating value, 43 070 J/g (18 530 Btu/lb).]

Mean working pressure	Cooling-water inlet temperature	Heater-tube gas temperature	Working-gas cold-space temperature	Engine output	Fuel flow	Engine GSFC
SI units						
MPa	°C	°C	°C	kW	g/h	g/kW · hr
6.89	61	706	130	6.00	2272	379
5.52	55	702	116	4.81	1914	398
4.14	48	700	102	3.50	1538	439
2.93	43	694	90	2.10	1211	577
2.07	39	683	82	1.03	962	934
1.23	36	680	74	0	739	---
U.S. customary units						
psig	°F	°F	°F	hp	lb/hr	lb/hp · hr
1000	142	1302	266	8.04	5.01	0.623
800	131	1296	240	6.45	4.22	.654
600	119	1292	215	4.69	3.39	.723
425	109	1282	194	2.82	2.67	.946
300	102	1262	179	1.38	2.12	1.536
178	96	1256	166	0	1.63	-----

TABLE A-II. - SYSTEM TESTS OF JUNE 1966

[Working fluid, hydrogen; operating speed, 3000 rpm; fuel, Dn; fuel lower heating value, 43 070 J/g (18 530 Btu/lb).]

Mean working pressure	Cooling-water inlet temperature	Heater-tube gas temperature	Alternator output		Alternator efficiency	Engine output	Fuel flow	System SFC	Engine BSFC	
SI units										
MPa	°C	°C	V	A	kW	percent	kW	g/hr	g/kW · hr	g/kW · hr
4.90	54	643	30	100	3.00	79.0	3.797	1901	634	501
4.36	52	654	30	90	2.70	79.5	3.396	1774	657	522
3.56	49	663	30.1	71	2.14	80.0	2.871	1560	729	584
2.83	48	666	30.3	49.5	1.50	80.0	1.875	1379	919	735
2.10	48	666	30.6	26	.796	78.0	1.021	1188	1492	1164
1.46	53	666	0	0	0	----	-----	1012	-----	-----
4.81	54	649	30.2	98	2.96	79.0	3.747	1869	631	499
4.83	56	649	30.3	99	3.00	79.0	3.797	1869	623	492
U.S. customary units										
psig	°F	°F	V	A	hp	percent	hp	lb/hr	lb/hp · hr	lb/hp · hr
710	130	1190	30	100	4.023	79.0	5.092	4.19	1.042	0.823
632	126	1210	30	90	3.621	79.5	4.555	3.91	1.080	.858
517	121	1225	30.1	71	2.866	80.0	3.583	3.44	1.200	.960
410	118	1230	30.3	49.5	2.012	80.0	2.515	3.04	1.511	1.209
305	118	1230	30.6	26	1.067	78.0	1.368	2.62	2.455	1.915
212	128	1230	0	0	0	----	-----	2.23	-----	-----
698	130	1200	30.2	98	3.969	79.0	5.024	4.12	1.038	.820
700	132	1200	30.3	99	4.023	79.0	5.092	4.12	1.024	.809

TABLE A-III. - SYSTEM TESTS OF JULY 1966

[Working fluid, hydrogen; operating speed, 3000 rpm; fuel, CITE; lower heating value, 43 070 J/g (18 530 Btu/lb).]

Mean working pressure	Cooling-water inlet temperature	Working-gas cold-space temperature	Heater-tube gas temperature	Alternator output			Alternator efficiency	Engine output	Fuel flow	System SFC	Engine BSFC
SI units											
MPa	°C	°C	°C	V	A	kW	percent	kW	g/hr	g/kW · hr	g/kW · hr
1.93	49	88	599	30	10	0.30	73.5	0.408	1293	4310	3169
1.97	47	85	593	↓	10	.30	73.5	.408	1279	4263	3135
2.72	52	102	607	↓	40	1.20	79.2	1.515	1497	1248	988
4.00	52	104	593	↓	75	2.25	80.0	2.813	1860	827	661
5.24	60	132	593	↓	100	3.00	79.0	3.797	2059	686	542
1.52	46	91	604	↓	0	----	----	----	1139	----	----
U. S. customary units											
psig	°F	°F	°F	V	A	hp	percent	hp	lb/hr	lb/hp · hr	lb/hp · hr
280	120	190	1110	30	10	0.402	73.5	0.547	2.85	7.089	5.210
285	117	185	1100	↓	10	.402	73.5	.547	2.82	7.015	5.155
395	125	215	1125	↓	40	1.609	79.2	2.031	3.30	2.051	1.625
580	125	220	1100	↓	75	3.016	80.0	3.770	4.10	1.359	1.088
760	140	270	1100	↓	100	4.021	79.0	5.090	4.54	1.129	.892
220	115	195	1120	↓	0	----	----	----	2.51	----	----

## REFERENCES

1. Heffner, F. Earl: Highlights from 6500 Hours of Stirling Engine Operation. SAE Paper 650254, Jan. 1965.
2. Percival, W. H.: Historical Review of Stirling Engine Development in the United States from 1960 to 1970. (Rept. 4-E8-00595, General Motors Research Labor.; Environmental Protective Agency Contract 4-E8-00595.) NASA CR-121097, 1974.
3. Meijer, R. J.: The Philips Stirling Thermal Engine. PhD. Thesis, Technical University Delft, 1960. (Also published as Philips Research Reports, Supplements No. 1, 1961, pp. 1-126.)
4. Davis, Stephen R.; Henein, Naeim A.; and Lundstrom, Richard R.: Combustion and Emission Formation in the Stirling Engine with Exhaust Gas Recirculation. SAE Paper 710824, Oct. 1971.
5. Davis, Stephen R.; and Henein, Naeim A.: Comparative Analysis of Stirling and Other Combustion Engines. SAE Paper 730620, July 1973.
6. Tew, Roy C., Jr.; Jefferies, Kent S.; and Miao, David: Stirling Engine Computer Model for Performance Calculations. NASA TM-78884, 1978.



ORIGINAL  
OF POOR QUALITY

ORIGINAL PAGE IS  
OF POOR QUALITY

TABLE I. - GPU 3 ENGINE DIMENSIONS AND PARAMETERS

Number of cylinders . . . . .	1
Type of engine . . . . .	Displacer
Drive . . . . .	Rhombic
Working fluid . . . . .	Hydrogen
Design speed, rpm . . . . .	3000
Design mean compression-space pressure, MPa (psig) . . . . .	6.89 (1000)
Design brake output power, kW (hp) . . . . .	6 (8)
Design heater-tube gas temperature, °C (°F) . . . . .	677 (1250)
Design cooling-water-inlet temperature, °C (°F) . . . . .	37 (100)
Cylinder bore, cm (in.) . . . . .	6.99 (2.75)
Stroke, cm (in.) . . . . .	3.15 (1.24)
Displacement (maximum change in total working space volume), cm <sup>3</sup> (in. <sup>3</sup> ) . . . . .	119.6 (7.30)
Displacer rod diameter, cm (in.) . . . . .	0.953 (0.375)
Piston rod diameter, cm (in.) . . . . .	2.223 (0.875)
Cooler:	
Tube length, cm (in.) . . . . .	4.470 (1.76)
Heat-transfer length, cm (in.) . . . . .	3.480 (1.37)
Tube inside diameter, cm (in.) . . . . .	0.102 (0.040)
Tube outside diameter, cm (in.) . . . . .	0.152 (0.060)
Number of tubes per cylinder . . . . .	312
Number of tubes per cooler . . . . .	39
Heater:	
Mean tube length, cm (in.):	
Regenerator side . . . . .	12.90 (5.08)
Cylinder side . . . . .	11.63 (4.58)
Heat-transfer length, cm (in.) . . . . .	7.772 (3.06)
Tube inside diameter, cm (in.) . . . . .	0.302 (0.119)
Tube outside diameter, cm (in.) . . . . .	0.483 (0.190)
Number of tubes per cylinder . . . . .	80
Regenerators:	
Length (inside), cm (in.) . . . . .	2.260 (0.89)
Diameter (inside), cm (in.) . . . . .	2.260 (0.89)
Number per cylinder . . . . .	8
Matrix:	
Wire cloth material . . . . .	304 stainless steel
Cloth mesh, per 2.5 cm (1 in.) . . . . .	200 by 200
Wire diameter, μm (in.) . . . . .	40.64 (0.0016)
Number of layers . . . . .	308
Filler factor, percent . . . . .	28.6
Drive:	
Connecting rod length, cm (in.) . . . . .	4.597 (1.81)
Crank radius, cm (in.) . . . . .	1.379 (0.543)
Eccentricity, cm (in.) . . . . .	2.083 (0.82)

TABLE II. - INSTRUMENTATION ORIGINALLY SUPPLIED WITH GPU 3

Item	Parameter	Instrument	Range
1	Hydrogen bottle pressure	Gage	0 - 3000 psig
2	Hydrogen supply pressure	Gage	0 - 1500 psig
3	Oil pump pressure	Gage	0 - 100 psig
4	Compression-space mean pressure	Gage	0 - 1000 psig
5	Buffer-space mean pressure	Gage	0 - 1500 psig
6	Nozzle fuel pressure	Gage	0 - 15 psig
7	Engine oil pressure	Gage	0 - 100 psig
8	Fuel pump pressure	Gage	0 - 30 psig
9	Heater-tube gas temperature (2)	Thermocouple	0 - 1500 <sup>o</sup> F
10	Compression-space temperature	Thermocouple	0 - 500 <sup>o</sup> F
11	Oil sump temperature	Thermocouple	0 - 500 <sup>o</sup> F
12	Water-inlet temperature	Thermocouple	0 - 500 <sup>o</sup> F
13	Alternator output voltage	Voltmeter	0 - 30 V dc
14	Alternator output current	Ammeter	0 - 150 A
15	Buffer-space gas temperature	Thermocouple	0 - 500 <sup>o</sup> F
16	Engine speed (not operable)	dc generator	2600 - 3200 rpm

TABLE III. - INSTRUMENTATION ADDED TO GPU 3

Item	Parameter	Instrument	Range
17	Water-outlet temperature	Thermocouple	0 - 500 <sup>o</sup> F
18	Preheater air-inlet temperature	Thermocouple	0 - 500 <sup>o</sup> F
19	Combustion-blower outlet pressure	Gage	0 - 35 in water
20	Fuel nozzle atomizing air pressure	Gage	0 - 15 psig
21	Governor oil control signal pressure	Gage	0 - 60 psig
22	Cooling-water supply pressure	Gage	0 - 15 psig
23	Engine speed	Pulse type with frequency meter	-----

TABLE IV. - LEWIS GPU 3 TEST DATA WITH HYDROGEN WORKING FLUID

[Operating speed, 3000 rpm; fuel, No. 1 diesel; fuel lower heating value, 43 197 J/g (18 584 Btu/lb).]

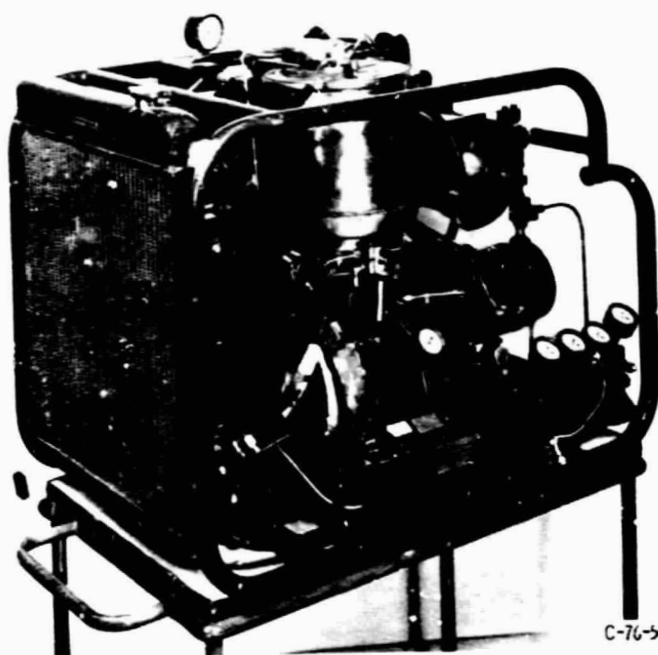
Mean working pressure	Heater-tube gas temperature	Alternator output		Alternator efficiency	Engine output	Fuel flow	System SFC	Engine BSFC	
SI units									
MPa	°C	V	A	kW	percent	kW	g/hr	g/kW · hr	g/kW · hr
1.74	674	29.0	0	0	----	-----	872	-----	-----
1.86	671	29.0	6	.174	72.4	0.240	799	4592	3329
1.93	674	29.5	11	.325	73.7	.441	872	2683	1977
2.05	674	29.5	16	.487	75.0	.649	1024	2100	1578
2.31	677	29.5	26	.767	77.2	.994	1068	1392	1074
2.71	674	29.0	36	1.044	78.6	1.238	1084	1019	801
3.00	677	29.3	46	1.348	79.0	1.706	1236	917	725
3.36	677	29.3	55	1.612	80.0	2.015	1304	809	647
3.90	674	29.5	69	2.036	80.3	2.535	1476	725	582
4.45	677	29.1	81	2.357	80.0	2.946	1576	669	535
5.00	677	28.5	91	2.594	79.3	3.271	1768	682	541
U. S. customary units									
psig	°F	V	A	hp	percent	hp	lb/hr	lb/hp · hr	lb/hp · hr
252.5	1245	29.0	0	0	----	-----	1.922	-----	-----
270	1240	29.0	6	.233	72.4	0.292	1.762	7.562	5.472
280	1245	29.5	11	.435	73.7	.590	1.922	4.418	3.256
297.5	1245	29.5	16	.652	75.0	.869	2.257	3.462	2.597
335	1250	29.5	26	1.028	77.2	1.232	2.354	2.290	1.767
392.5	1245	29.0	36	1.399	78.6	1.780	2.346	1.677	1.318
435	1250	29.3	46	1.807	79.0	2.287	2.725	1.508	1.192
487.5	1250	29.3	55	2.160	80.0	2.700	2.875	1.331	1.065
565	1245	29.5	69	2.729	80.3	3.399	3.254	1.192	.957
645	1250	29.1	81	3.160	80.0	3.950	3.474	1.099	.879
725	1250	28.5	91	3.477	79.3	4.365	3.996	1.121	.889

TABLE V. - LEWIS GPU 3 TEST DATA WITH HELIUM WORKING FLUID

[Operating speed, 3000 rpm; fuel, No. 1 diesel; fuel lower heating value, 43 197 J/g (18 584 Btu/lb).]

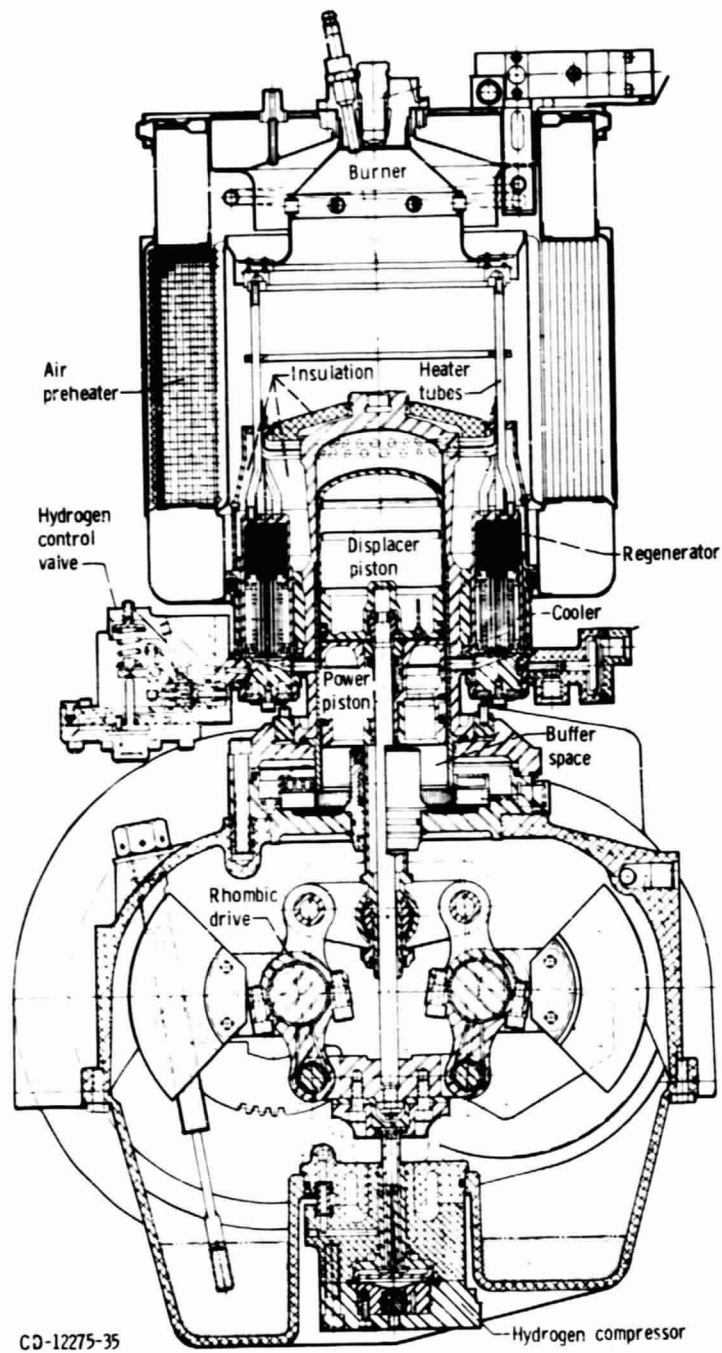
Mean working pressure	Cooling-water inlet temperature	Heater-tube gas temperature	Alternator output		Alternator efficiency	Engine output	Fuel flow	system SFC	Engine BSFC	
SI units										
MPa	°C	°C	V	A	kW	percent	kW	g/hr	g/kW · hr	g/kW · hr
2.69	27	671	28.5	0	0	----	-----	1136	-----	-----
2.81	28	677	29.0	7	.20	72.8	0.279	1160	5714	4158
3.09	32	679	29.0	12	.348	73.9	.471	1197	3440	2541
3.33	29	677	29.0	17	.493	75.3	.655	1296	2629	979
3.67	32	682	29.0	27	.783	77.4	1.012	1436	1834	1419
4.22	37	679	29.0	36	1.044	78.9	1.323	1508	1444	1140
5.02	43	677	29.0	46	1.334	79.5	1.678	1700	1274	1013
U. S. customary units										
psig	°F	°F	V	A	hp	percent	hp	lb/hr	lb/hp · hr	lb/hp · hr
390	80	1240	28.5	0	0	----	-----	2.504	-----	-----
407.5	82	1250	29.0	7	.272	72.8	0.374	2.557	9.401	6.837
447.5	90	1255	29.0	12	.466	73.9	.631	2.640	5.773	4.184
482.5	85	1250	29.0	17	.661	75.3	.878	2.697	4.322	3.254
532.5	90	1260	29.0	27	1.050	77.4	1.356	3.166	3.015	2.335
612.5	98	1255	29.0	36	1.399	78.9	1.773	3.325	2.377	1.874
727.5	109	1250	29.0	46	1.788	79.5	2.249	3.748	2.096	1.667

ORIGINAL PAGE IS  
OF POOR QUALITY



C-76-569

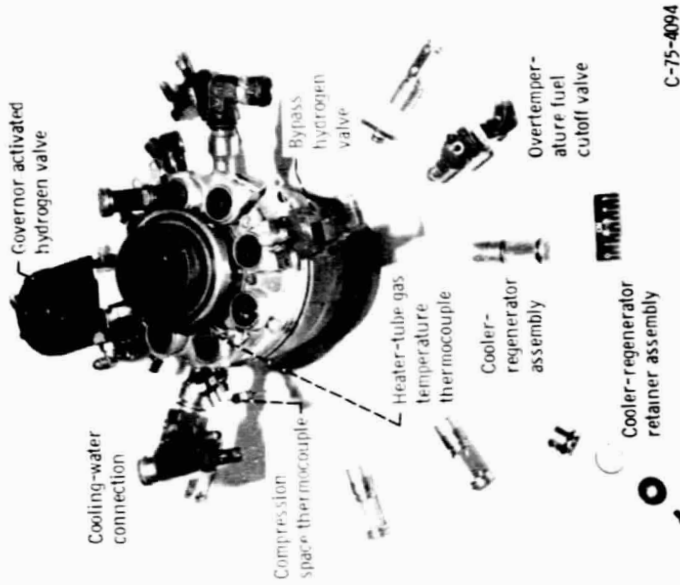
Figure 1. - GPU 3 Stirling ground power unit.



CD-12275-35

Figure 2. - Cross section of GPU 3 engine.

ORIGINAL PAGE IS  
OF POOR QUALITY



(a) Assembled.

(b) Partially disassembled.

Figure 3. - GPU cylinder assembly.

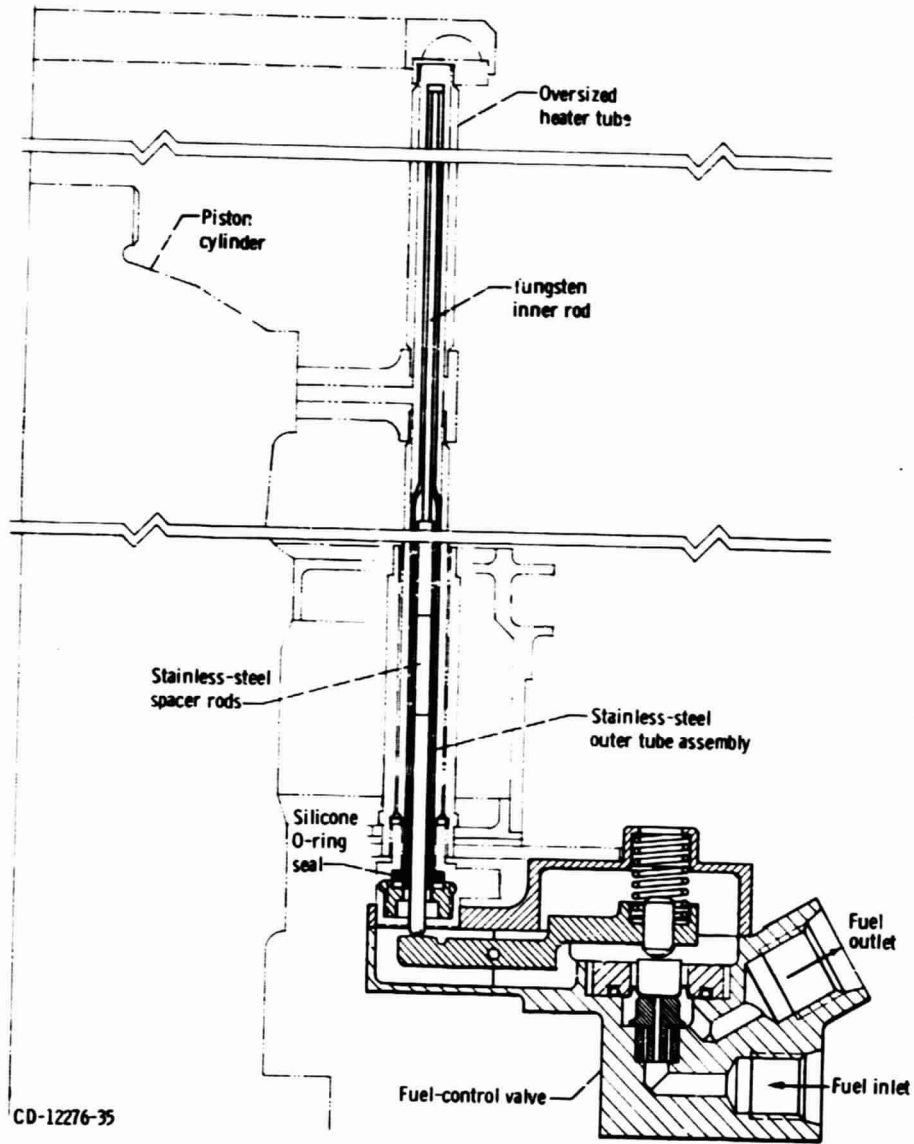
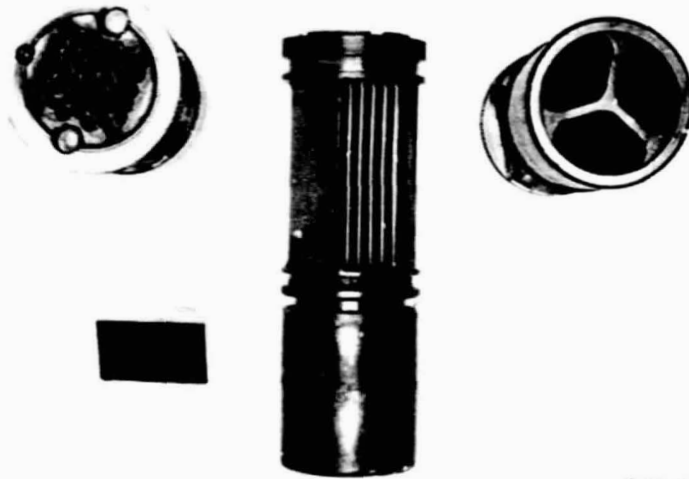


Figure 4 - Temperature-activated fuel-control valve.

ORIGINAL PAGE IS  
OF POOR QUALITY



C-75-4103

Figure 5. - Cooler-regenerator cartridge assembly.



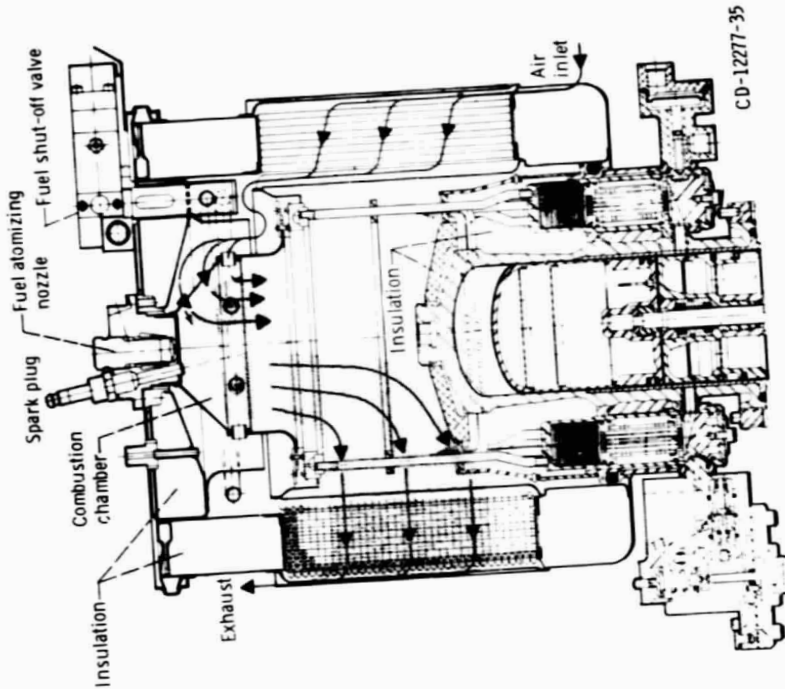


Figure 6. - Air preheater and combustor assembly.

ORIGINAL PAGE IS  
OF POOR QUALITY

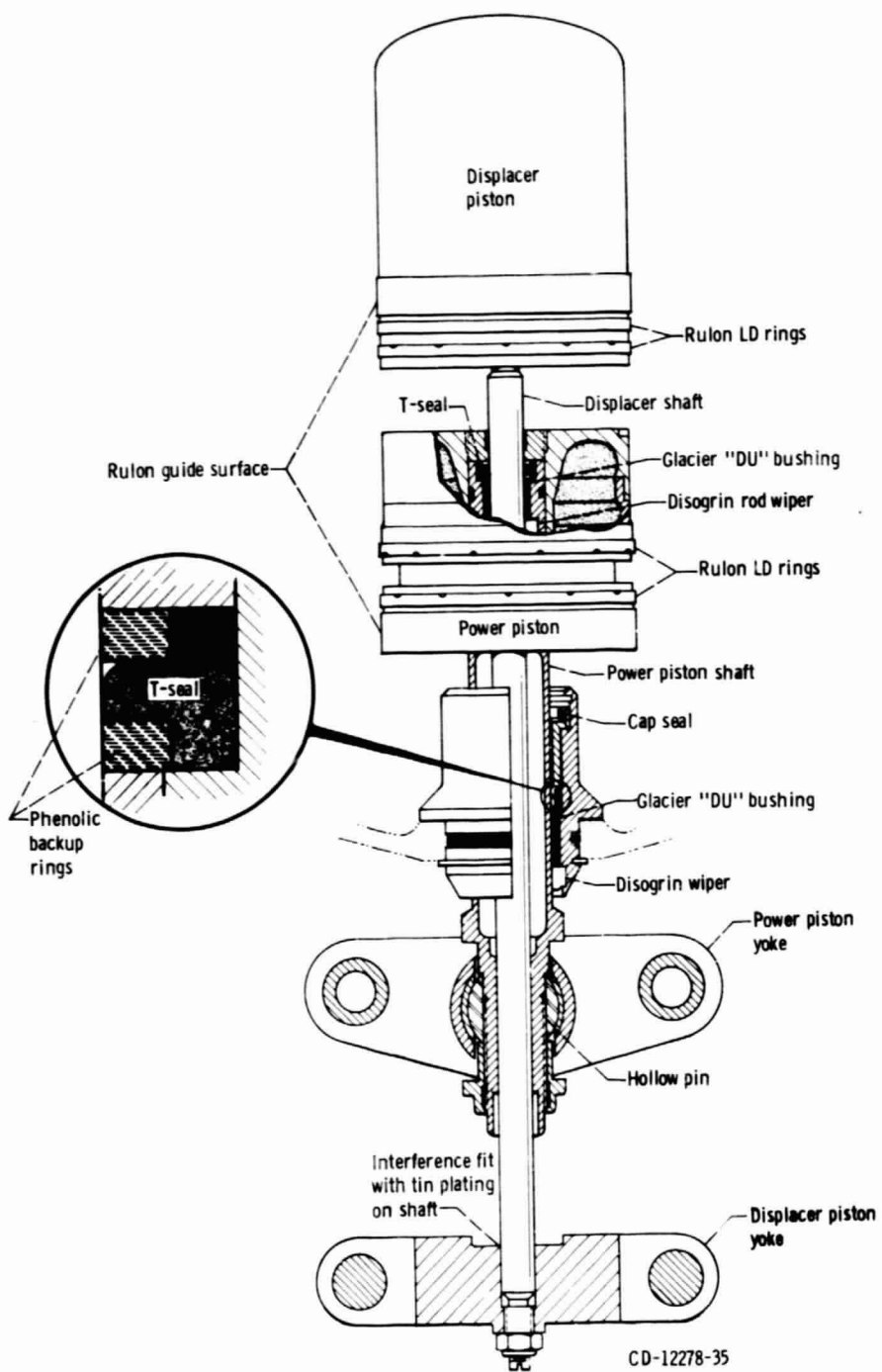


Figure 7. - GPU 3 pistons, shafts, and seals assembly.

**ORIGINAL PAGE IS  
OF POOR QUALITY**



Figure 8. - Displacer shaft and seal parts.

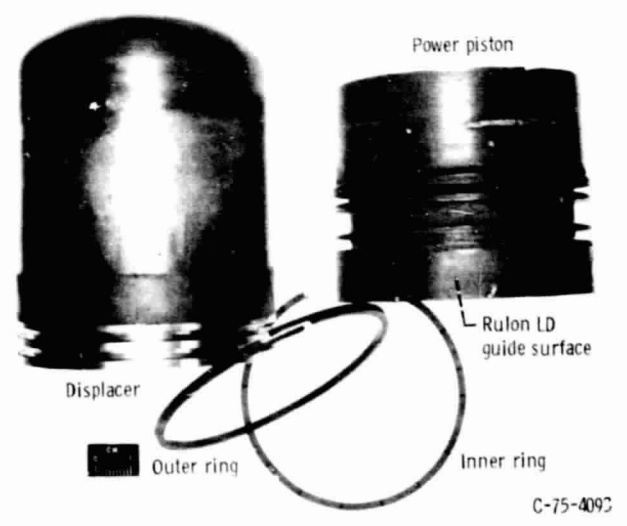


Figure 9. - GPU 3 Pistons and piston rings.

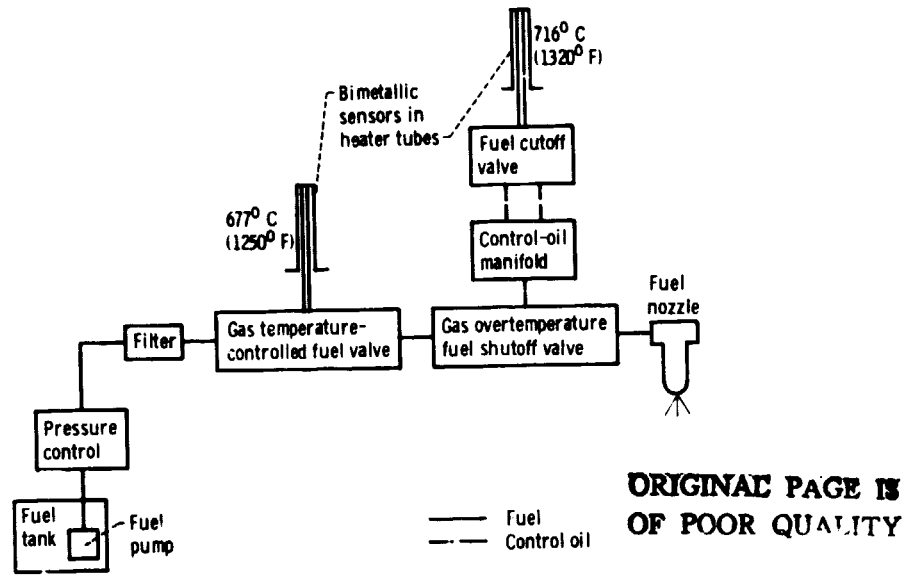


Figure 10. - Heater-tube temperature control, simplified schematic.

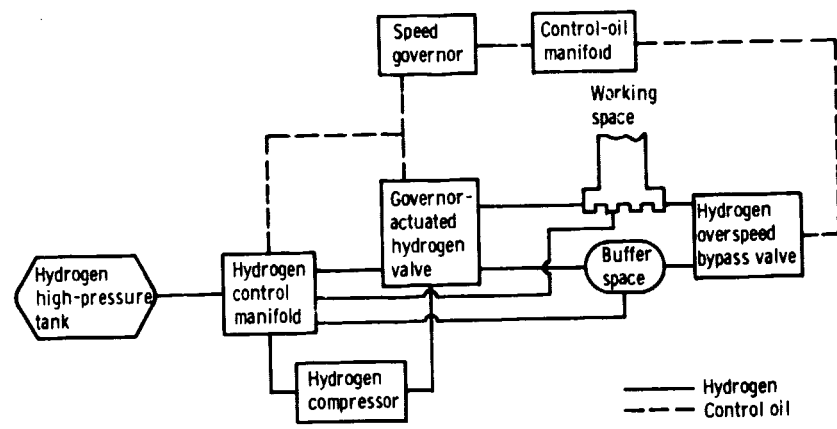


Figure 11. - Engine speed control, simplified schematic.

**ORIGINAL PAGE IS  
OF POOR QUALITY**

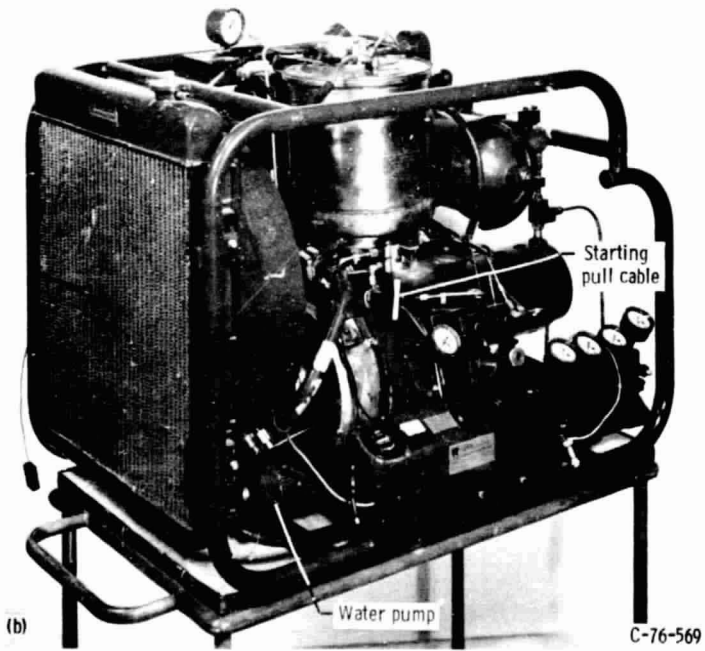
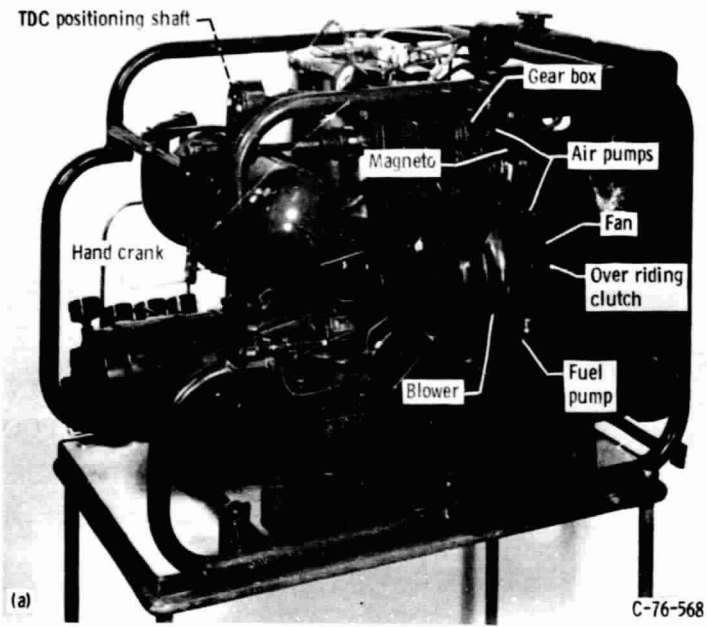


Figure 12. - GPU 3 as-received at Lewis.

ORIGINAL PAGE IS  
OF POOR QUALITY

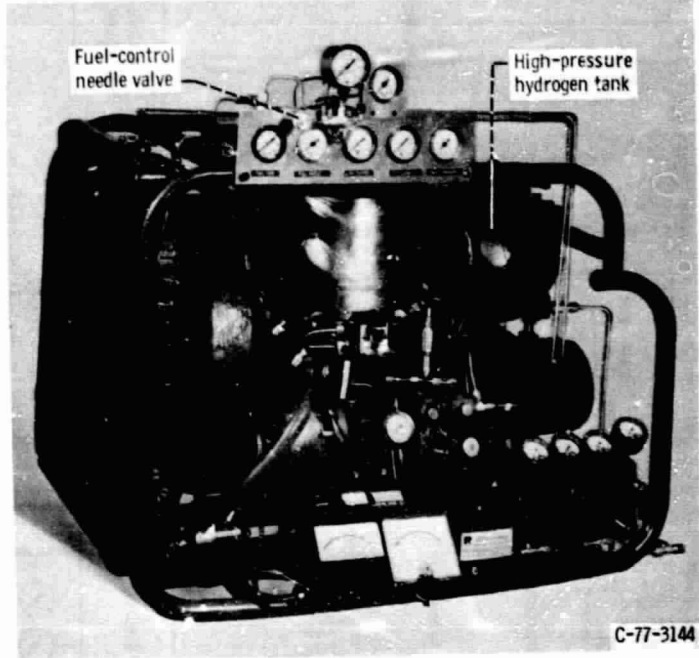


Figure 13. - GPU as tested.

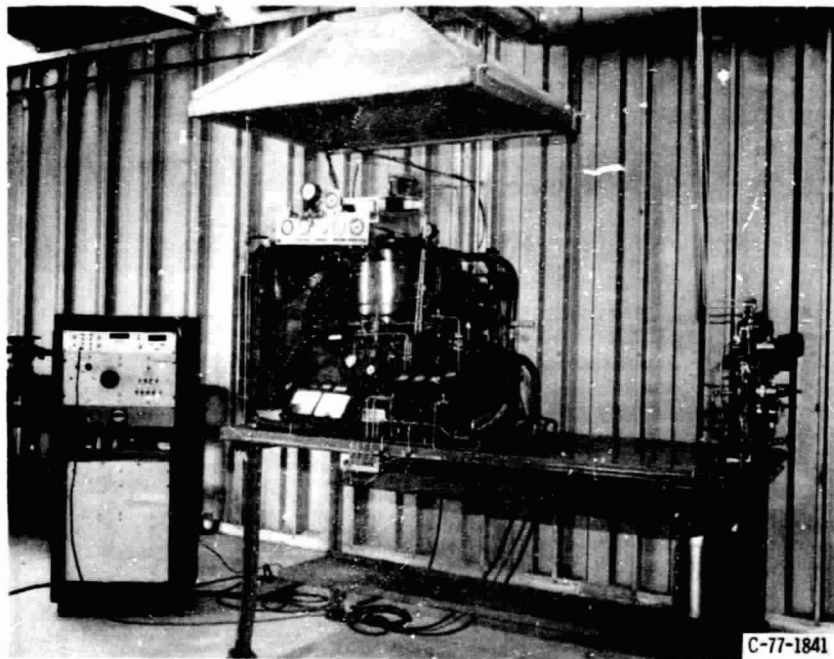


Figure 14. - GPU 3 test setup.



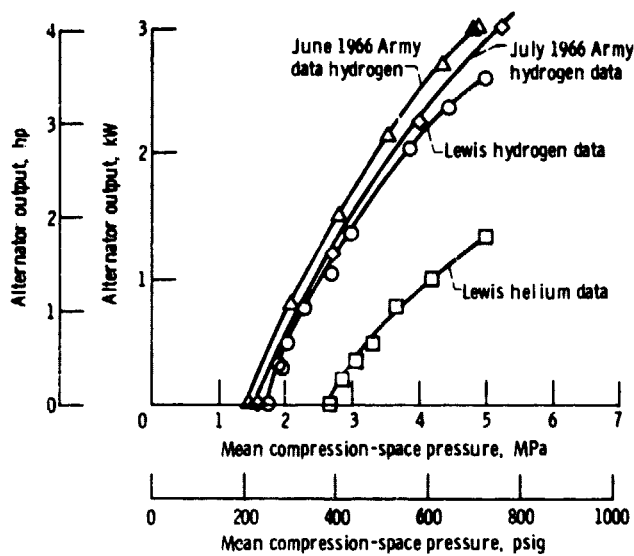


Figure 16. - GPU 3 alternator output versus mean working pressure at 3000 rpm.

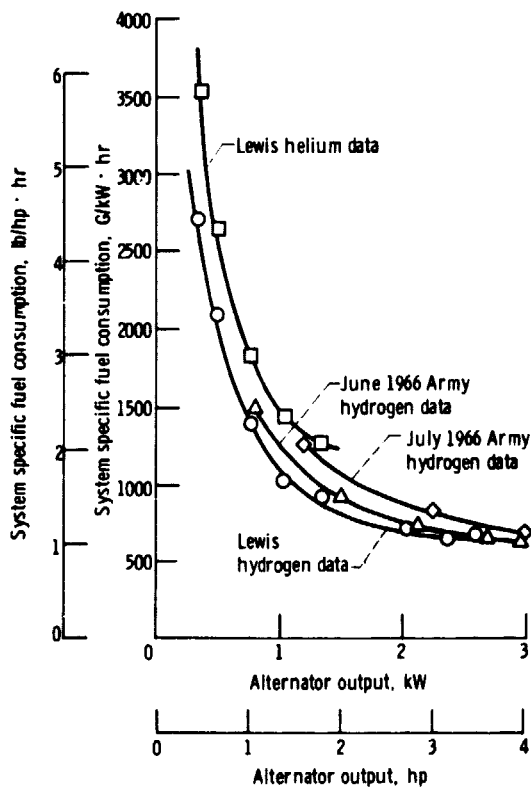


Figure 17. - GPU 3 system specific fuel consumption versus alternator output at 3000 rpm.



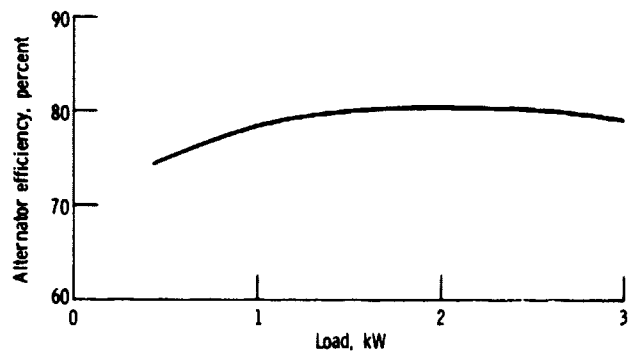


Figure 18. - Alternator efficiency versus load at 30 volts and 3000 rpm.

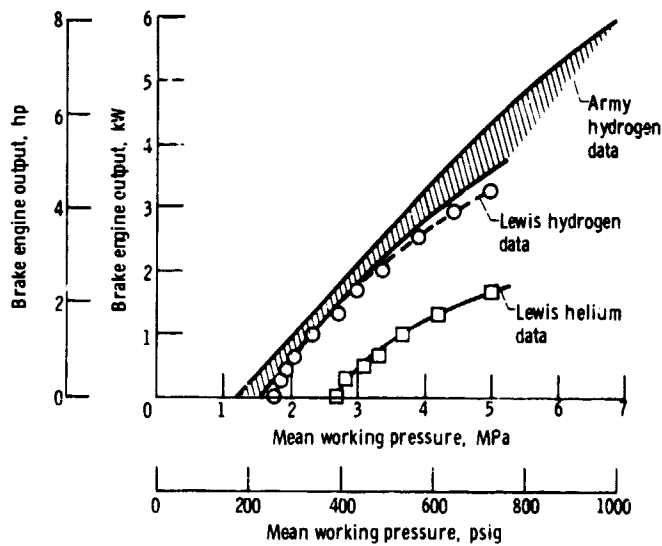


Figure 19. - GPU 3 engine output versus mean working pressure.

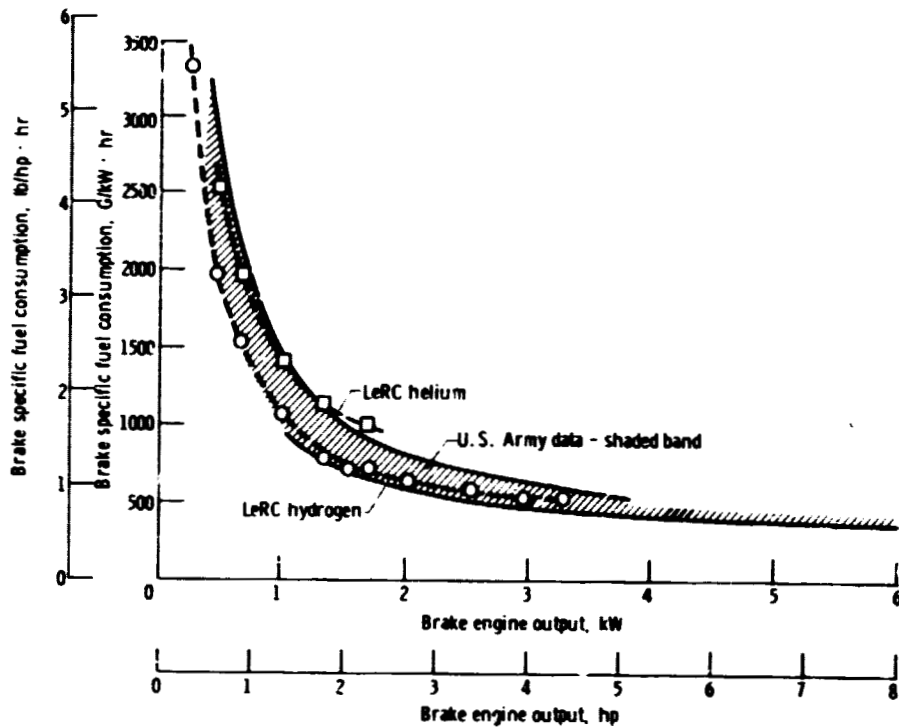


Figure 20. - GPU 3 specific fuel consumption versus engine output.